Supporting Information

rAAV8-mediated inhibition of miRNA-21 protects mice against the lethal schistosome infection by repressing both IL-13 and TGF-β1 pathways

Xing He, Jun Xie, Dongmei Zhang, Qin Su, Xue Sai, Ruipu Bai, Chao Chen, Xufeng Luo, Guangping Gao, Weiqing Pan

Supporting Materials and Methods

LNA-based miRNA microarray analysis. Total RNA was harvested using TRIzol (Invitrogen) according to manufacturer's instructions. After having passed RNA measurement on the Nanodrop instrument, the samples were labeled using the miRCURY™ Hy3™/Hy5™ Power labeling kit and hybridized on the miRCURY™ LNA Array (v.14.0). Scanning was performed with the Axon GenePix 4000B microarray scanner. GenePix pro V6.0 was used to read the raw intensity of the image. The results were subjected to unsupervised hierarchical clustering (Cluster 3.0).

Real-time PCR and Northern blot analysis. The assay was performed as described previously.[1] The expression of miR-21, miR-223, miR-146a, miR-146b, miR-203, miR-365, Col1α1, Col3α1, TGF-β1, IL-13 and SMAD7 was determined using the SYBR Green Master Mix kit (Takara, Kusatsu, Japan). U6 snRNA or GAPDH was used as an internal control, and the fold change was calculated by the 2-[delta][delta] Ct method. The sequences of the primers were shown in Supporting Table 1. Northern blot was performed as described previously.[2]

Liver histopathology and fibrosis measurement. The number of schistosome eggs in the liver was counted after the liver tissue was digested by 4% KOH. Liver egg burdens were expressed as 10^4 eggs per gram of liver tissue. The liver index was calculated as the following formula: (the total weight of mouse liver / the total weight of mouse body)×100%. The size of egg granulomas was measured from Mayer's H&E sections using a calibrated measuring eyepiece. The maximal and minimal diameters of granulomas and the number of granulomas in each section were measured. The granuloma area was calculated by multiplying the maximal and minimal diameters of granuloma, and the mean area of granulomas was calculated as the following formula: the total area of all granulomas in each section / the number of granulomas in each section. The collagen content of the liver, determined as hydroxyproline content, was

detected using a colourmetric assay according to manufacturer's instructions (Nanjing Jiancheng Bioengineering Institute, Nanjing, China). Fibrosis was also scored histologically using liver sections stained with Masson's trichrome staining as described previously.[3] All granulomas within each section were scored for blue density on a scale of 1–4, and a second measurement of area involved was also determined using the same scale. The total fibrosis score was determined by multiplying the density and area for each granuloma (a score of 16 would be the maximum).

In situ hybridization (ISH). The assay was performed as described previously.[4] In brief, liver sections were incubated with 50nM Digoxigenin (Dig)-conjugated miR-21 probes (Exiqon) or Dig-conjugated control probes with scrambled sequence (Exiqon) at 50°C for 1 hour, and HRP-conjugated anti-Dig antibody (Roche) was used to display the signals.

Isolation of mouse HSCs, hepatocytes and Kuppfer cells. Liver was initially *in situ* digested with 0.04% collagenase type IV and then further digested with 0.08% collagenase type IV at 37°C bath shaking for 30 minutes. Hepatocytes were isolated by centrifugation of the resulting cell suspension at 50g for 4 minutes and further purified by centrifugation at 20g for 4 minutes. After hepatocytes were pelleted, the supernatant containing nonparenchymal cells was further centrifuged at 500g for 5 minutes. HSCs were isolated from nonparenchymal cells using 11.5% (w/v) iodixanal gradient (OptiPrep; Axis-Shield PoC AS, Oslo, Norway) at 1400g for 20 minutes. To further purify HSCs, we depleted HSCs of Kupffer cells by magnetic antibody cell sorting (MACS, MiltenyiBiotec) with CD11b-conjugated microbeads (MiltenyiBiotec). The purity of HSCs was higher than 95% evaluated by retinoid autofluorescence. Kuppfer cells were first separated from nonparenchymal cells by centrifugation on a 25%-50% Percoll gradient at 900g for 20 minutes. The Kupffer-cell fraction located at the interface of the 25%-50% Percoll layer. CD11b positive cells (referred to as Kupffer cells in this study) were then purified using positive selection with magnetic CD11b

antibody beads and magnetic columns (MACS, Miltenyi, Auburn, CA). FACS-Calibur analysis demonstrated >90% purity after labeling purified cells with CD11b-FITC antibody (Miltenyi; Auburn, CA).

Cell culture and treatment. Primary HSCs were cultured on plastic dishes in DMEM, supplemented with 4 mmol/L L-glutamine, 10% FCS, and penicillin (100 IU/ml)/streptomycin (100 mg/ml). The first medium change was performed 24 h after seeding. Cells were maintained at 37°C, 5% CO_2 in a humidified atmosphere. HSCs were exposed to recombinant TGF-β1 (PEPROTECH) or IL-13 (PROSPEC) at day 3 after starvation overnight with 0.5% FCS, and harvested at appointed time points. SMAD7 or EGFP plasmid transfection was performed on HSCs at day 2 after seeding using Lipofectamine 2000 (Invitrogen).

Construction of plasmids and vectors. β-Gal gene was PCR amplified from plasmid pAAV2.1TBGLacZ [5] using primer claczF with Nhe I site and claczR with Xho I site. PCR fragment was cut with these two restriction enzymes and cloned into Nhe I and Xho I sites in psiCHECK plasmid. Three copies of perfectly complementary miR-21 sites were designed based on the annotated miR-21 inserted between the Xho I and Not I restriction sites after β-Gal gene to make pmiCHECK-21 sensor plasmid. To express miR-21, a pri-miR-21 fragment was amplified from mouse genome DNA using primer pri-miR-21F and pri-miR-21R and cloned into PpuMI site in pAAVscCBPIpGluc plasmid. BamH I digested anti-miR-21 TuD fragment (synthesized from Gensript) was cloned into BamH I site in pAAVscCBPITuDlet-7pGluc after anti-let-7 TuD was removed. rAAV8 vectors used in the study were produced, purified and tittered as described. [6]

Western blotting. Total cell protein was extracted on ice with RIPA lysis buffer in the presence of freshly added protease and phosphatase inhibitors (Thermo), and quantified by the BCA method (Pierce). A total of 30 μg / lane protein extract was loaded onto a

12% SDS-polyacrylamide gel and transferred to nitrocellulose membranes (Pierce). Nonspecific binding was blocked with 5% nonfat milk in TBST. The membrane was incubated with rabbit anti-SMAD7 (Abcam, Cat. MAB2029), anti-phospho-SMAD1/5 (Cell signaling, Cat. 41D10), anti-phospho-SMAD2 (Cell signaling, Cat. 138D4), or anti-phospho-SMAD3 (Cell signaling, Cat. C25A9) antibody overnight at 4°C. IRDye 800CW goat anti-rabbit IgG (LI-COR, Cat. 926-32211) was used as secondary antibody, and rabbit anti-GAPDH antibody (EPITOMICS, Cat. 2251-1) was used as an internal standard.

Detection of IL-4 / IFN-γ, ALT and LPS in serum. Levels of IL-4 and IFN-γ in serum were determined using commercial enzyme-linked immune sorbent assay (ELISA Kits, BioLend Inc., USA). ALT and LPS levels in serum were detected using a colourmetric assay according to manufacturer's instructions (TECO DIAGNOSTICS, USA; Chinese Horseshoe Crab Reagent Manufactory Co., Ltd., China).

Ex vivo intracellular cytokine staining. Leukocytes isolated from spleen were stimulated with PMA (50ng/mL), Ionomycin (1 μg/mL) and BFA (3μg/mL) for 5 hours. Cells were surface stained with PerCP/Cy5.5 conjugated CD3 and APC conjugated CD4, permeabilized with 0.1% spaonin buffer for 15 minutes, and further stained with FITC conjugated IFN-γ and PE conjugated IL-4 before acquiring with FACS Calibur. Antibodies were from BioLend Inc.. Data were analyzed in Flowjo.

Statistics. Results are reported as mean ± s.d. and compared between groups using two-tailed Student's t- test, one-way ANOVA or Kaplan-Meier method. Data were considered statistically significant for P values less than 0.05.

Supporting Results

Anti-miR-21-TuD mediated down-regulation of miR-21.

To validate the potency and specificity of anti-miR-21-TuD, in addition to the anti-miR-21-TuD expressing construct, we constructed two more control vectors: 1). a miR-21 sensor construct carrying a firefly luciferase (Fluc) reporter gene as an internal control for transfection efficiency and the β-galactosidase (β-Gal) gene that is regulated by 3 copies of miR-21 target sites as a miR-21 sensor, and 2). a pri-miR-21 overexpression construct (Supporting Fig. 2A). MiR-21 sensor construct was co-transfected with anti-miR-21-TuD construct into HEK293 cells, activities of β-Gal and Fluc in the cellular lystes were measured 24 hours later by bioluminescent assays and presented as ratios of β-Gal and Fluc activities which reflect the levels of active miR-21 in the transfected cells. Our data revealed, in the absence of anti-miR-21-TuD, a 70% reduction of Fluc activity with miR-21 sensor plasmid as compared to the control, suggesting that the presence of endogenous miR-21 in 293 cells causes repression of Fluc activity expressed from miR-21-sensor construct (Supporting Fig. 2B). However, co-transfection with as low as 5 ng of anti-miR-21-TuD construct can initiate derepression of miR-21 sensor by inhibiting endogenous miR-21 in 293 cells, which reaches the maximum rescue (>70%) of miR-21 sensor with 125 ng of TuD DNA (Supporting Fig. 2B, top panel). To verify the specificity of anti-miR-21-TuD-mediated derepression of miR-21 sensor, we co-transfected 293 cells with pri-miR-21 expressing, miR-21 sensor and anti-miR-21-TuD constructs into HEK293 cells. Addition of pri-miR-21 dramatically lowered the β-Gal / Fluc ratio from 0.31 ± 0.02 to 0.02 ± 0.004, suggesting ectopic expression of functional miR-21 in 293 cells; yet increasing amounts of anti-miR-21-TuD plasmid effectively rescued the sensor from miR-21 specific silencing (Supporting Fig. 2B).

Supporting Figure Legends

Supporting Fig. 1. Deregulated miRNAs in the progression of hepatic schistosomiasis. In this experiment, mice were infected with 16 *S. japonicum* cercariae or remained uninfected. Liver samples of infected mice were collected at days 10, 26, 35, 42, 48, 56, 70 and 84 days post-infection (Ed10 to Ed84). Control liver samples were obtained from uninfected mice on days 26 (Cd26) and 70 (Cd70) of the experiment. Three mice were killed at each time point. Total RNA was extracted to analyze the alteration of miRNA expression profiles. (A) Hierarchical cluster analysis of the result of miRNA microarray. The liver samples of three mice collected at each time point (i.e. Ed10 to Ed84 for the infected mice and Cd 26 and Cd70 for the control mice) were mixed for microarray analysis. Bright green, under-expression; black, no change; bright red, over-expression. (B) List of deregulated miRNAs in the array analysis. (C) Real-time PCR validation of the expression of representative miRNAs. *, $P < 0.05$; **, $P < 0.01$; ***, $P < 0.001$ compared with Ed10.

Supporting Fig. 2. *In vitro* validation of the potency and specificity of anit-miR-21-TuD. (A) Construction of plasmids. (B) Top panel: miR-21 sensor plasmid was co-transfected with anti-miR-21 TuD plasmid into HEK293 cells, activities of β-Gal and Fluc in the cellular lystes were measured 24 hours later by bioluminescent assays and presented as ratios of β-Gal and Fluc activities which reflect the levels of active miR-21 in the transfected cells. Bottom panel: Pri-miR-21 expressing, miR-21 sensor and anti-miR-21-TuD constructs were co-transfected into HEK293 cells, and the activities of β-Gal and Fluc in the cellular lystes were measured 24 hours later.

Supporting Fig. 3. Sequestering miR-21 prevents hepatic schistosomiasis in mice. (A) Levels of miR-122 expression in liver samples determined using RT-PCR. (B) H&E staining of liver sections. Scale bar, 200 μm. (C) Mean area of granuloma measured from Mayer's H&E staining liver sections using a calibrated measuring eyepiece. (D) Recovered parasites from infected mice. (E) The number of schistosome eggs in the liver was counted after the liver tissue was digested by 4% KOH. (F) Liver index was

performed. (G) Transduced vector genomes of the livers were detected by real-time PCR. (H) Gluc activities in the serum.

Supporting Fig. 4. Quantification of the miR-21 levels in the other organs from liver of mice after 56-day infection, including heart (A), muscle (B), kidney (C), lung (D), pancreas (E), spleen (F), and brain (G).

Supporting Fig. 5. Effect of sequestering miR-21 on immune response and schistosomiasis-caused damage. In this experiment, mice were infected percutaneously with 16 *S. japonicum* cercariae at day 0 or remained uninfected. Infected mice received either 1×10^{12} virus genomes or PBS by tail injection at day 10 post-infection. Spleen and blood serum samples were obtained at day 35, 42, and 49 post-infection. Figures show levels of (A) ALT and (B) LPS in blood serum, and ELISA results for (C) IFN-γ and (D) IL-4. The minimum detectable concentration of IFN-γ and IL-4 for the ELISA kits was 15.6 pg/mL and 2 pg/mL, respectively. (E, F and G) The frequency of intracellular IFN-γ and IL-4 stained CD4+ T cells in the spleen.

Supporting Fig. 6. The expression level of TNF-α (A), IL-10 (B) and IL-5 (C) in the liver tissues from the 4 groups described in Fig. S5.

Supporting Fig. 7. Sequestering miR-21 partially reversed the hepatic schistosomiasis. (A) Masson's trichrome and HE staining of liver sections. Scale bar, 200 μm. (B) Liver index was performed. (C) The number of schistosome eggs in the liver was counted after the liver tissue was digested by 4% KOH. (D) Transduced vector genomes of the livers were detected by real-time PCR.

Supporting Fig. 8. No effect of the miR-21 level on production of TGF-β1 in both HSC and DC lines. HSC-T6 cell line was transfected with 80 nM miR-21 mimics or

inhibitor for 48 hours, and then the miR-21 (A), Smad7 (B), collagen (C) and TGF-β1 (D) expression level was detected by real-time PCR. (E) DC2.4 cell line was transfected with 80 nM miR-21 mimics or inhibitor for 24 hours, then was stimulated with 20μg/mL SEA for 12 hours. TGF-β1 expression level was detected by real-time PCR. miR-21: transfected with miR-21 mimics; anti-miR-21: transfected with anti-miR-21(inhibitor); NC: transfected with scramble miRNA; Mock: transfected with lipofectamine only.

Supporting Fig. 9. MiR-21 regulates the profibrogenic activities of TGF-β1 and IL-13 *in vivo*. (A) Collagen levels in HSCs. (B, C) Levels of SMAD7 in HSCs detected by Western blot. (D) Transduced vector genomes of the HSCs were detected by real-time PCR.

Supporting Fig. 10. Scheme of TGF-β1- and IL-13-induced miR-21 expression and its roles in HSCs. Schistosome infection increases the expression of the TGF-β1 and IL-13. Both molecules bind to their corresponding receptors to activate Smad proteins that are required for the processing of pri-miR-21 into pre-miR-21 by the DROSHA complex. The elevated expression of miR-21 then prompts Smad protein-dependent collagen production and fibrogenesis by relieving the inhibitory effect of SMAD7 on the SMAD signaling.

Supporting References

1. Chen C, Ridzon DA, Broomer AJ, Zhou Z, Lee DH, Nguyen JT, et al. Real-time quantification of microRNAs by stem-loop RT-PCR. Nucleic Acids Res 2005;33:e179.

2. Xie J, Ameres SL, Friedline R, Hung JH, Zhang Y, Xie Q, et al. Long-term, efficient inhibition of microRNA function in mice using rAAV vectors. Nat Methods 2012;9:403-409.
3. Chiaramonte MG, Donaldson DD, Cheever AW, Wynn TA. An IL-13 inhibitor blocks the development of hepatic fibrosis during a T-helper type 2-dominated inflammatory response. J Clin Invest 1999;104:777-785.
4. Jørgensen S, Baker A, Møller S, Nielsen BS. Robust one-day in situ hybridization protocol for detection of microRNAs in paraffin samples using LNA probes. Methods 2010;52:375-381.
5. Auricchio A, Hildinger M, O'Connor E, Gao GP, Wilson JM. Isolation of highly infectious and pure adeno-associated virus type 2 vectors with a single-step gravity-flowcolumn. Hum Gene Ther 2001;12:71-76.
6. Gao GP, Alvira MR, Wang L, Calcedo R, Johnston J, Wilson JM. Novel adeno-associated viruses from rhesus monkeys as vectors for human gene therapy. Proc Natl Acad Sci U S A 2002;99:11854-11859.

A

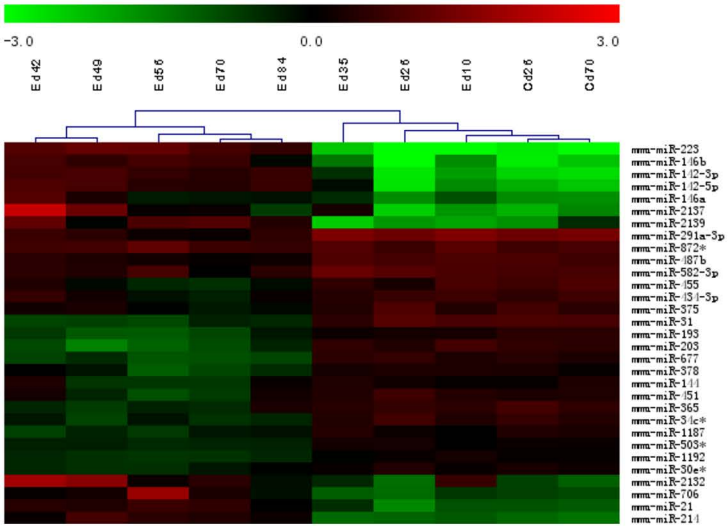

B

Up-regulated miRNAs (n=24)		Down-regulated miRNAs (n=9)	
miRNA	maximal fold change	miRNA	maximal fold change
miR-21	3.8	miR-802	-2.7
miR-146b	8.4	miR-203	-3.1
miR-142-3p	7.9	miR-31	-3.0
miR-223	19.9	miR-193	-2.1
miR-142-5p	8.1	miR-365	-2.2
miR-146a	4.6	miR-34c*	-2.5
miR-199a-3p	5.0	miR-770-5p	-2.8
miR-214	2.7	miR-451	-2.7
miR-706	5.9	miR-375	-2.1
miR-2132	6.4		
miR-2137	3.7		
miR-2135	5.5		
miR-2134	2.1		
miR-29b	2.5		
miR-195	2.8		
miR-199a-5p	4.3		
miR-33	2.5		
miR-34a	2.2		
miR-148b	2.1		
miR-351	2.6		
miR-301a	2.0		
miR-710	2.5		
miR-882	3.0		
miR-30b*	2.0		

C

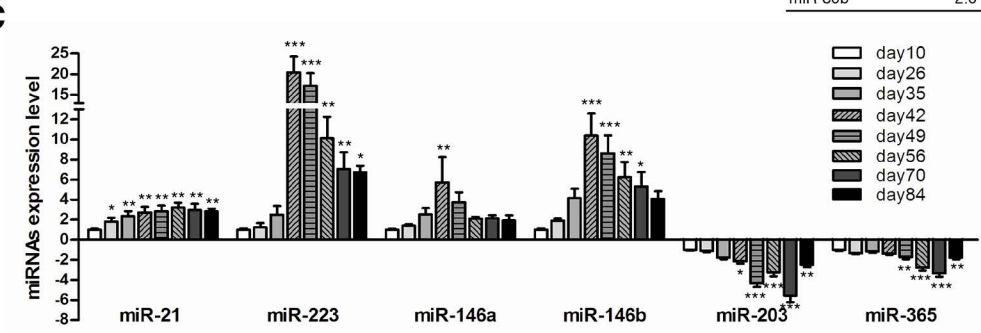

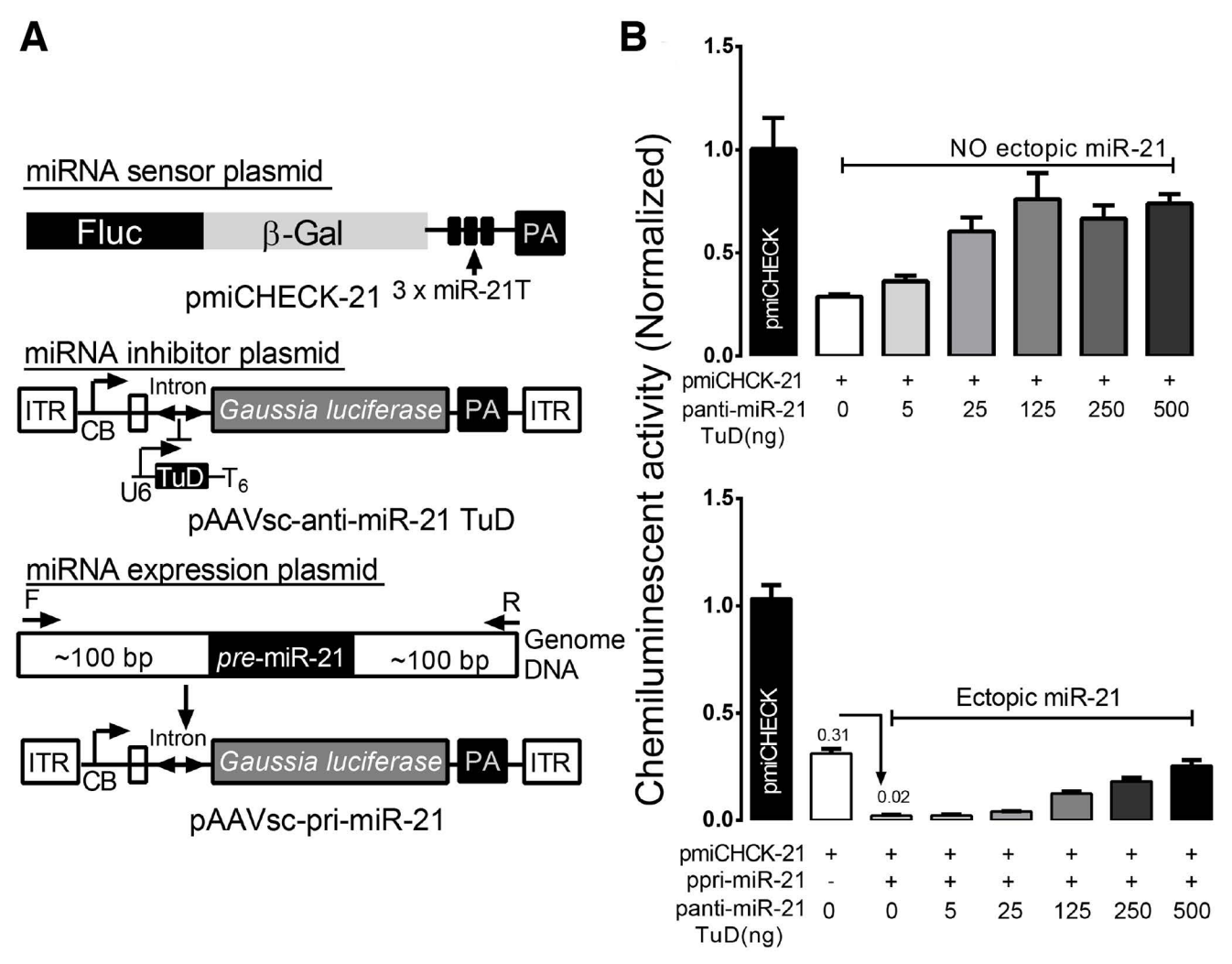
A
miRNA sensor plasmid
Fluc
β-Gal
PA
pmiCHECK-21
3 x miR-21T
miRNA inhibitor plasmid
ITR
Intron
CB
Gaussia luciferase
PA
ITR
U6
TuD
T6
pAAVsc-anti-miR-21 TuD
miRNA expression plasmid
F
R
~100 bp
pre-miR-21
~100 bp
Genome DNA
ITR
Intron
CB
Gaussia luciferase
PA
ITR
pAAVsc-pri-miR-21
B
Chemiluminescent activity (Normalized)
1.5
1.0
0.5
0.0
pmiCHECK
NO ectopic miR-21
pmiCHCK-21 + + + + + +
panti-miR-21 TuD(ng) 0 5 25 125 250 500
1.5
1.0
0.5
0.0
pmiCHECK
0.31
0.02
Ectopic miR-21
pmiCHCK-21 + + + + + + +
ppri-miR-21 - + + + + + +
panti-miR-21 TuD(ng) 0 0 5 25 125 250 500

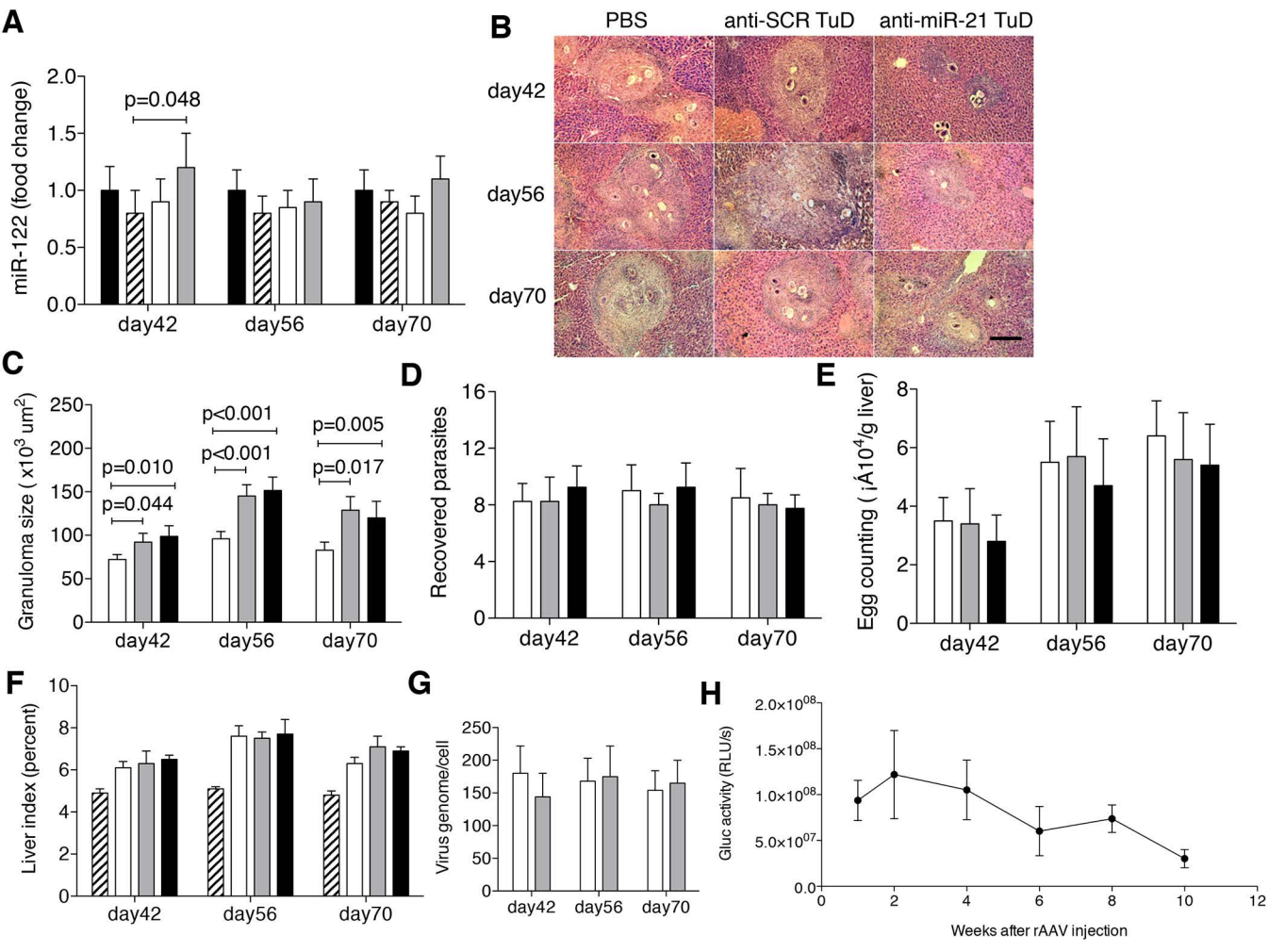
A
miR-122 (food change)
2.0
1.5
1.0
0.5
0.0
p=0.048
day42
day56
day70
B
PBS
anti-SCR TuD
anti-miR-21 TuD
day42
day56
day70
C
Granuloma size (x10^3 um^2)
250
200
150
100
50
0
p=0.010
p=0.044
p<0.001
p<0.001
p=0.005
p=0.017
day42
day56
day70
D
Recovered parasites
16
12
8
4
0
day42
day56
day70
E
Egg counting (iÁ10^4/g liver)
8
6
4
2
0
day42
day56
day70
F
Liver index (percent)
10
8
6
4
2
0
day42
day56
day70
G
Virus genome/cell
250
200
150
100
50
0
day42
day56
day70
H
Gluc activity (RLU/s)
2.0×10^08
1.5×10^08
1.0×10^08
5.0×10^07
0.0
0
2
4
6
8
10
12
Weeks after rAAV injection

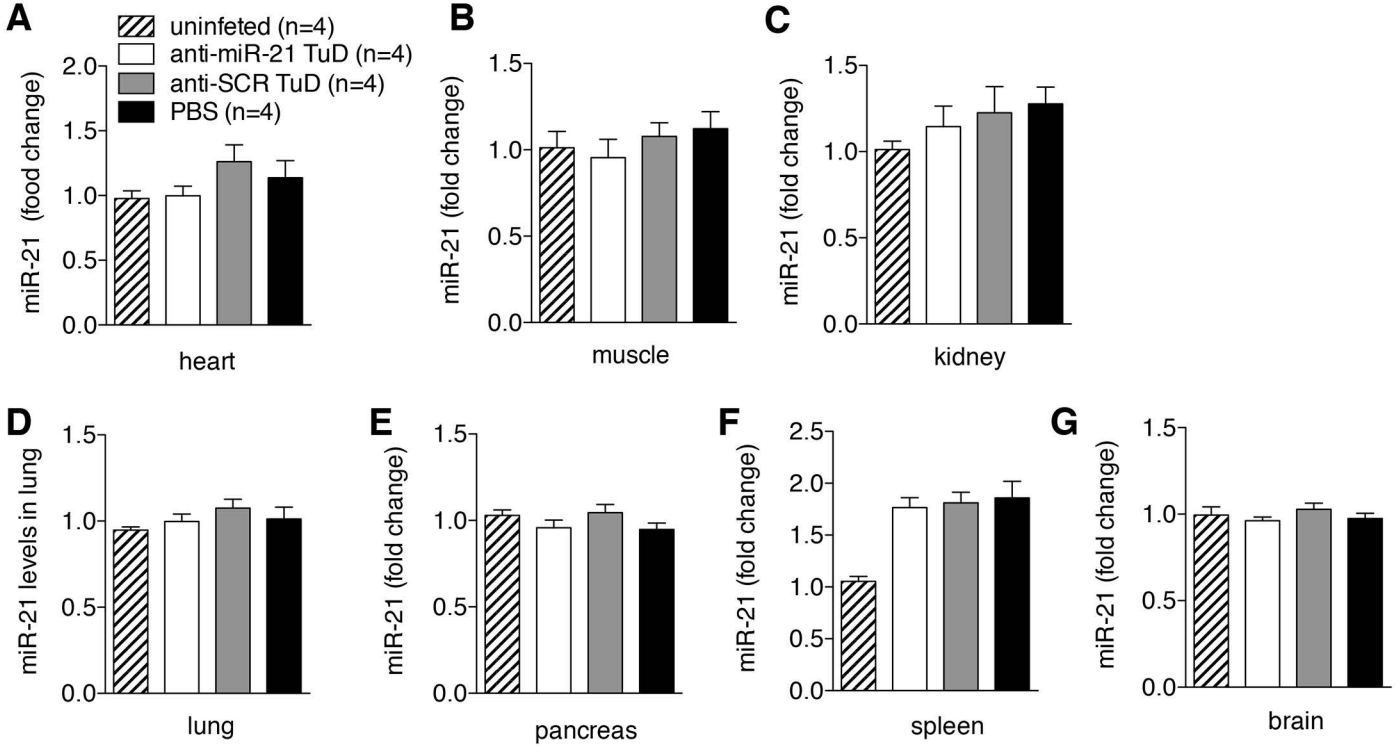
A
uninfeted (n=4)
anti-miR-21 TuD (n=4)
anti-SCR TuD (n=4)
PBS (n=4)
miR-21 (food change)
2.0
1.5
1.0
0.5
0.0
heart
B
miR-21 (fold change)
1.5
1.0
0.5
0.0
muscle
C
miR-21 (fold change)
1.5
1.0
0.5
0.0
kidney
D
miR-21 levels in lung
1.5
1.0
0.5
0.0
lung
E
miR-21 (fold change)
1.5
1.0
0.5
0.0
pancreas
F
miR-21 (fold change)
2.5
2.0
1.5
1.0
0.5
0.0
spleen
G
miR-21 (fold change)
1.5
1.0
0.5
0.0
brain

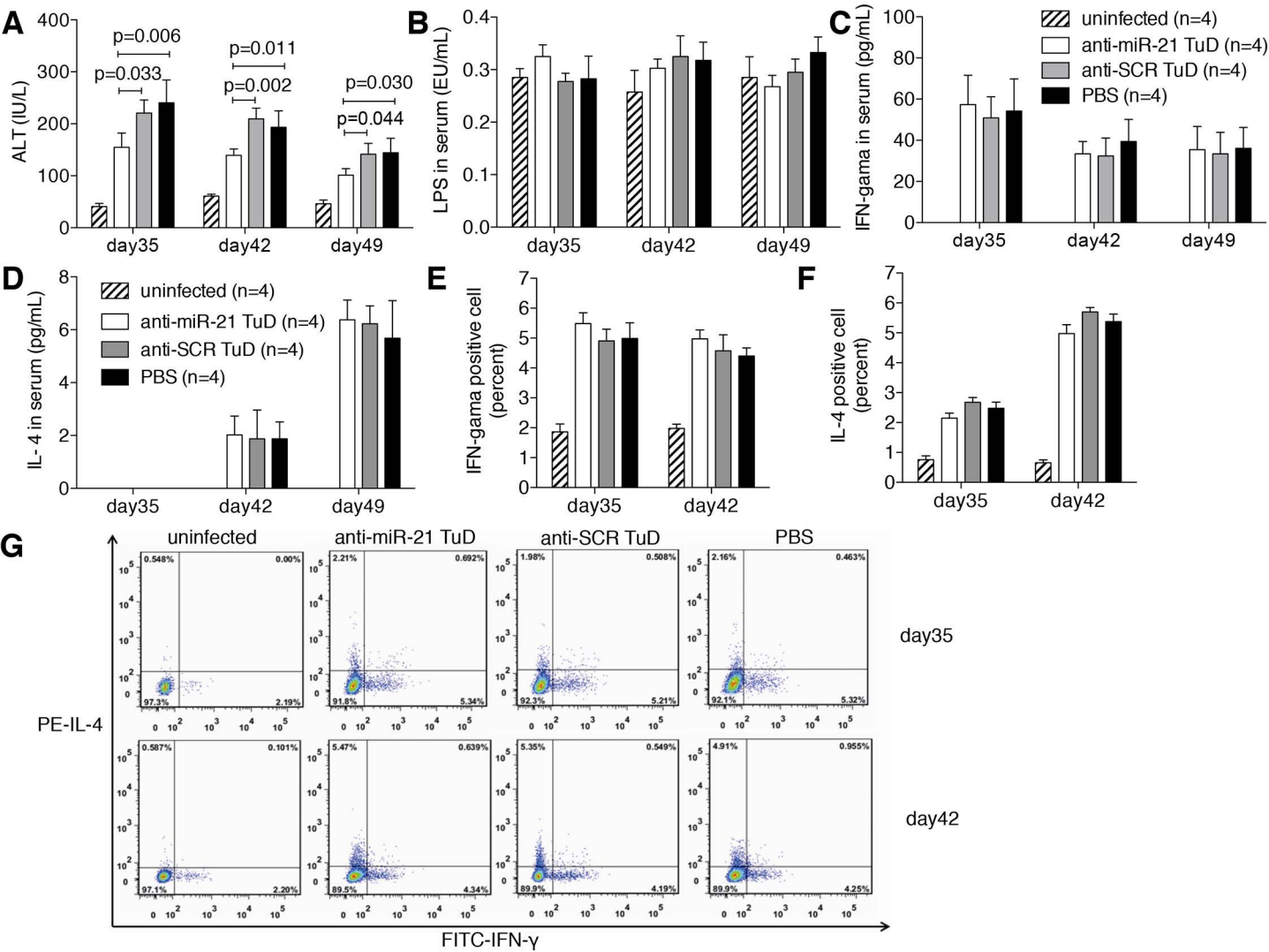
A
ALT (IU/L)
p=0.006
p=0.033
p=0.011
p=0.002
p=0.030
p=0.044
day35
day42
day49
B
LPS in serum (EU/mL)
C
IFN-gama in serum (pg/mL)
uninfected (n=4)
anti-miR-21 TuD (n=4)
anti-SCR TuD (n=4)
PBS (n=4)
D
IL- 4 in serum (pg/mL)
E
IFN-gama positive cell (percent)
F
IL-4 positive cell (percent)
G
uninfected
anti-miR-21 TuD
anti-SCR TuD
PBS
day35
day42
PE-IL-4
FITC-IFN-γ
0.548%
0.00%
97.3%
2.19%
2.21%
0.692%
91.8%
5.34%
1.98%
0.508%
92.3%
5.21%
2.16%
0.463%
92.1%
5.32%
0.587%
0.101%
97.1%
2.20%
5.47%
0.639%
89.5%
4.34%
5.35%
0.549%
89.9%
4.19%
4.91%
0.955%
89.9%
4.25%

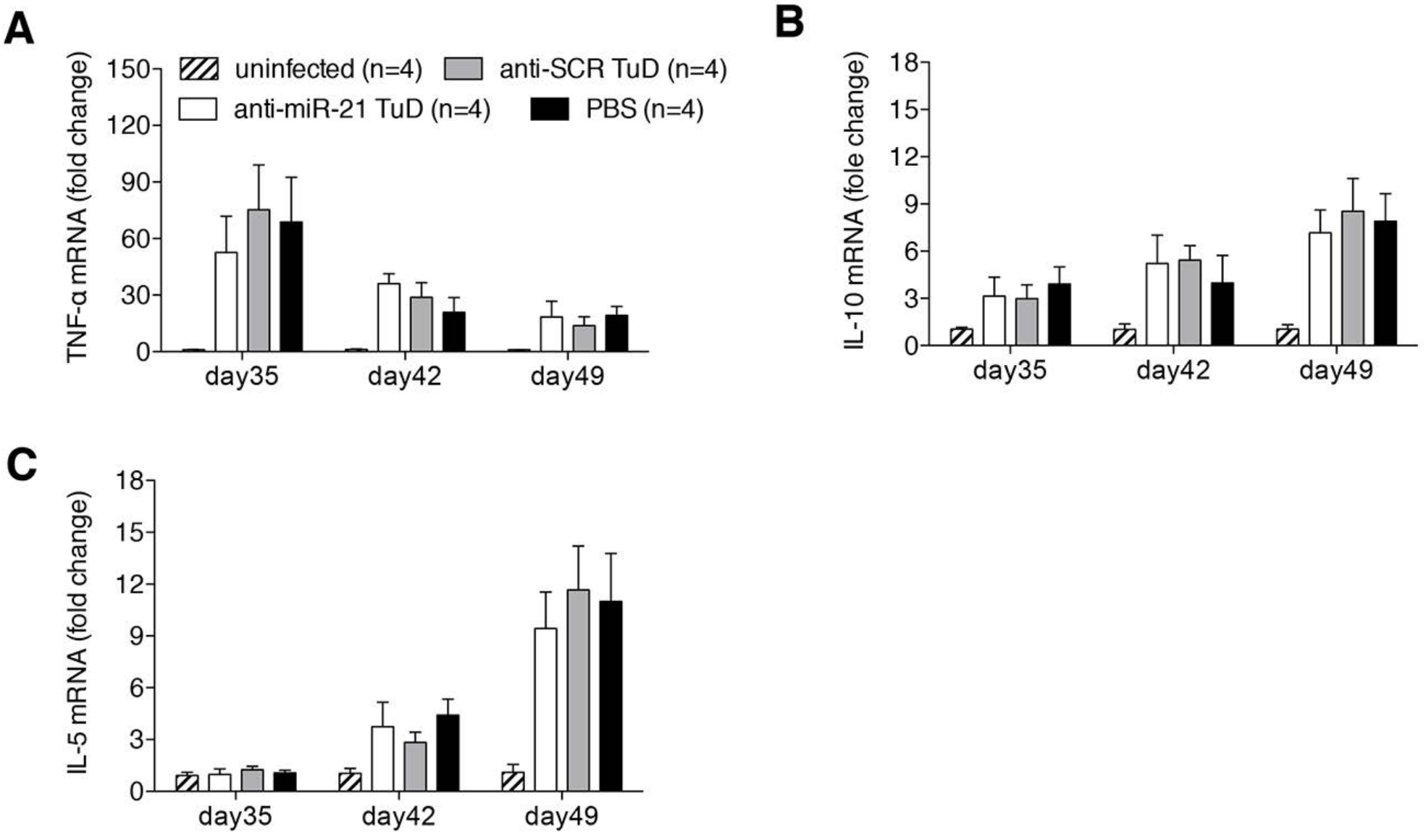
A
uninfected (n=4)
anti-SCR TuD (n=4)
anti-miR-21 TuD (n=4)
PBS (n=4)
TNF-α mRNA (fold change)
150
120
90
60
30
0
day35
day42
day49
B
IL-10 mRNA (fole change)
18
15
12
9
6
3
0
day35
day42
day49
C
IL-5 mRNA (fold change)
18
15
12
9
6
3
0
day35
day42
day49

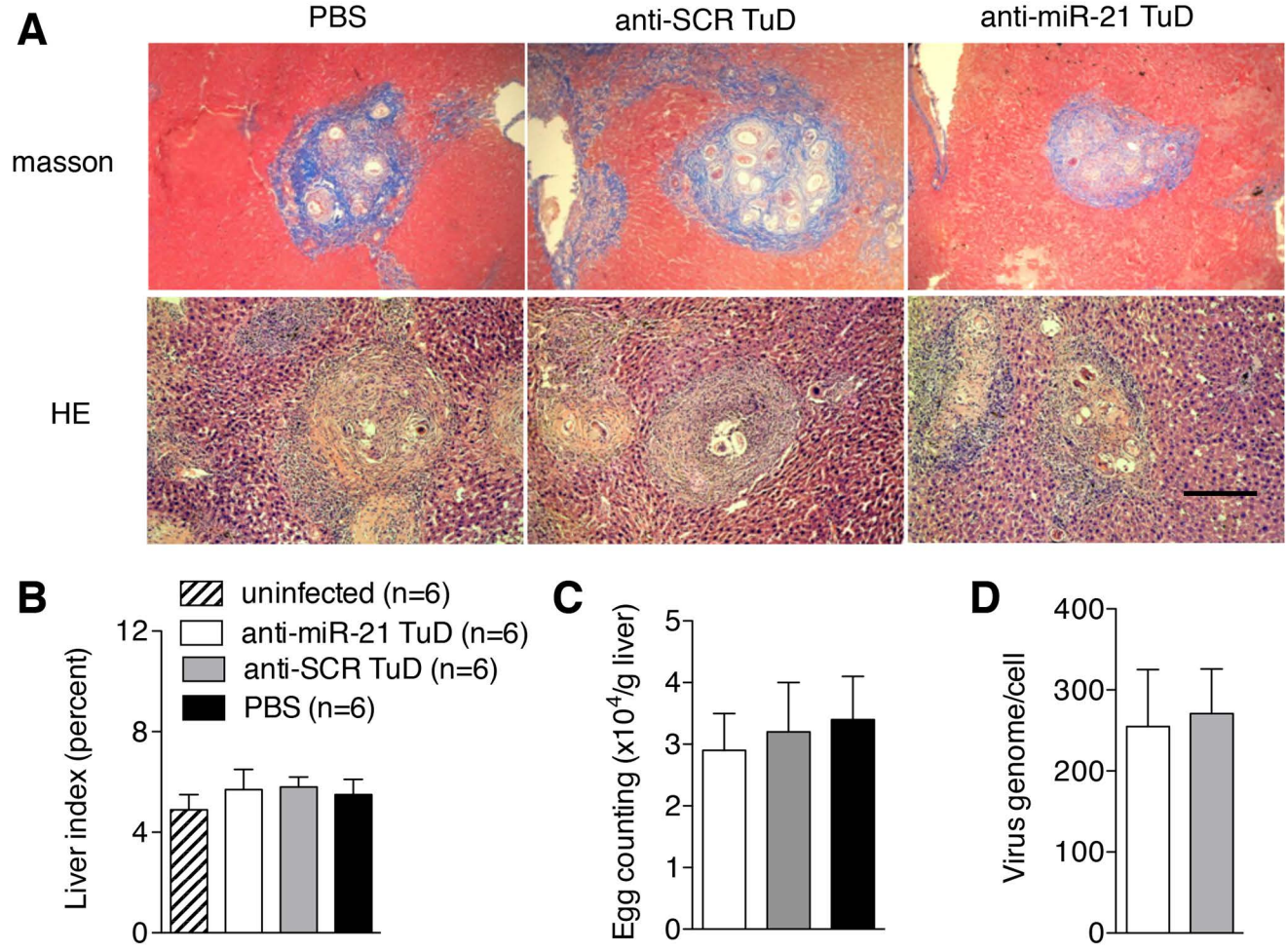
A
PBS
anti-SCR TuD
anti-miR-21 TuD
masson
HE
B
uninfected (n=6)
anti-miR-21 TuD (n=6)
anti-SCR TuD (n=6)
PBS (n=6)
Liver index (percent)
12
8
4
0
C
Egg counting (x10^4/g liver)
5
4
3
2
1
0
D
Virus genome/cell
400
300
200
100
0

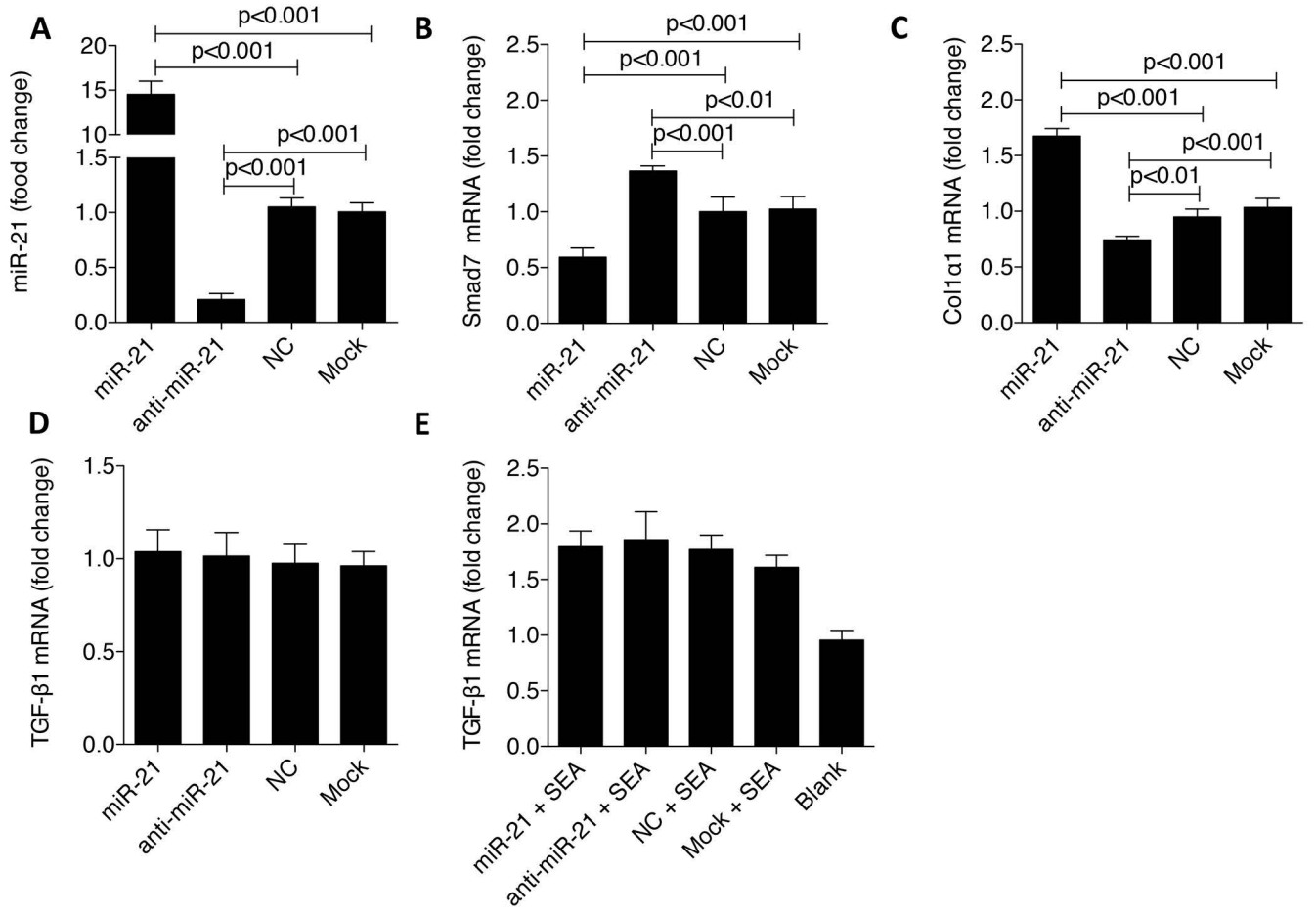
A
B
C
D
E
miR-21 (food change)
Smad7 mRNA (fold change)
Col1α1 mRNA (fold change)
TGF-β1 mRNA (fold change)
TGF-β1 mRNA (fold change)
p<0.001
p<0.001
p<0.001
p<0.001
p<0.001
p<0.01
p<0.001
p<0.001
p<0.01
p<0.001
miR-21
anti-miR-21
NC
Mock
miR-21 + SEA
anti-miR-21 + SEA
NC + SEA
Mock + SEA
Blank

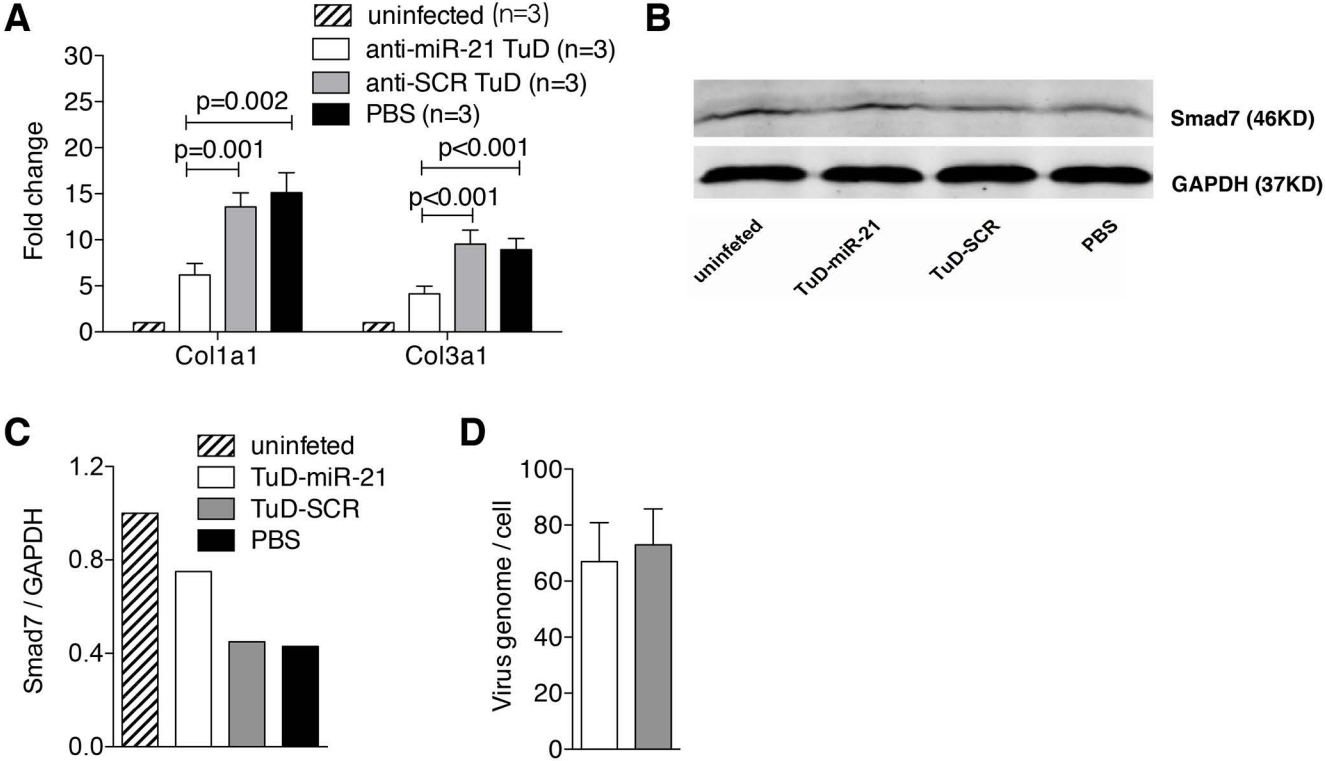
A
uninfected (n=3)
anti-miR-21 TuD (n=3)
anti-SCR TuD (n=3)
PBS (n=3)
Fold change
30
25
20
15
10
5
0
p=0.002
p=0.001
p<0.001
p<0.001
Col1a1
Col3a1
B
Smad7 (46KD)
GAPDH (37KD)
uninfeted
TuD-miR-21
TuD-SCR
PBS
C
uninfeted
TuD-miR-21
TuD-SCR
PBS
Smad7 / GAPDH
1.2
0.8
0.4
0.0
D
Virus genome / cell
100
80
60
40
20
0

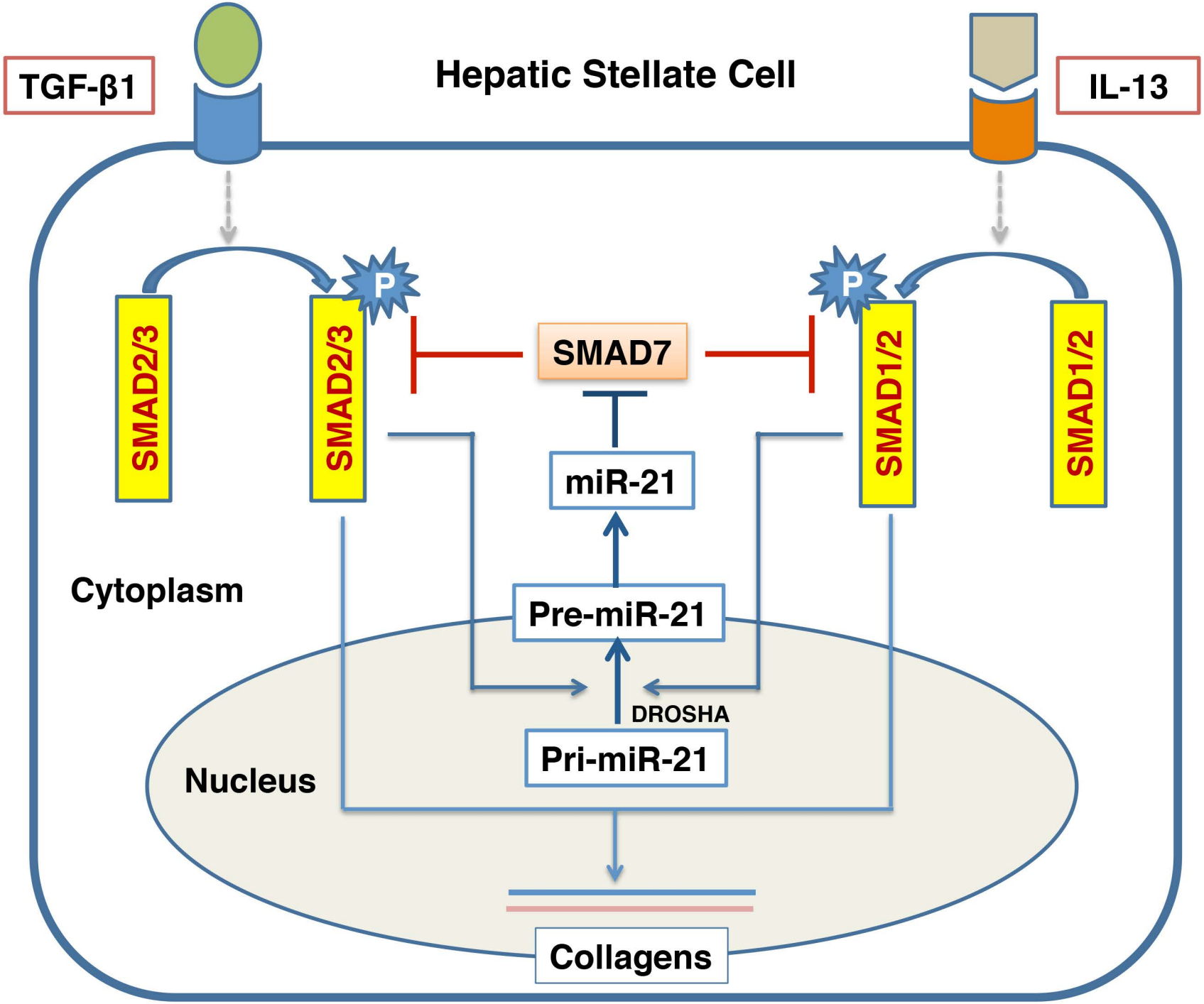
TGF-β1
Hepatic Stellate Cell
IL-13
SMAD2/3
P
SMAD2/3
SMAD7
P
SMAD1/2
SMAD1/2
miR-21
Cytoplasm
Pre-miR-21
DROSHA
Pri-miR-21
Nucleus
Collagens

Supporting Table 1. Primer sequences used in the study.

gene		primer sequence (5'→3')
miR-21	RT stem-loop primer	GTCGTATCCAGTGCAGGGTCCGAGGTATTCGCACTGGATACGACTCAACATC
	forward primer	ATGGTTCGTGGGTAGCTTATCAGACTGA
	reverse primer	GCAGGGTCCGAGGTATTC
miR-146a	RT stem-loop primer	GTCGTATCCAGTGCAGGGTCCGAGGTATTCGCACTGGATACGACAACCCATG
	forward primer	ATGGTTCGTGGGTGAGAACTGAATTCCA
	reverse primer	GCAGGGTCCGAGGTATTC
miR-146b	RT stem-loop primer	GTCGTATCCAGTGCAGGGTCCGAGGTATTCGCACTGGATACGACAGCCTATG
	forward primer	ATGGTTCGTGGGTGAGAACTGAATTCCA
	reverse primer	GCAGGGTCCGAGGTATTC
miR-223	RT stem-loop primer	GTCGTATCCAGTGCAGGGTCCGAGGTATTCGCACTGGATACGACTGGGGTAT
	forward primer	ATGGTTCGTGGG TGTCAGTTTGTCAAAT
	reverse primer	GCAGGGTCCGAGGTATTC
miR-203	RT stem-loop primer	GTCGTATCCAGTGCAGGGTCCGAGGTATTCGCACTGGATACGACCTAGTGGT
	forward primer	ATGGTTCGTGGGGTGAAATGTTTAGGAC
	reverse primer	GCAGGGTCCGAGGTATTC
miR-365	RT stem-loop primer	GTCGTATCCAGTGCAGGGTCCGAGGTATTCGCACTGGATACGACCACATCTG
	forward primer	ATGGTTCGTGGGAGGGACTTTTGGG
	reverse primer	GCAGGGTCCGAGGTATTC
U6	forward primer	GCTTCGGCAGCACATATACTAAAAT
	reverse primer	CGCTTCACGAATTTGCGTGTCAT
TGF-β1	forward primer	TGACGTCACTGGAGTTGTACGG
	reverse primer	GGTTCATGTCATGGATGGTGC
Col 1α1	forward primer	GCACGAGTCA CACCGGAAC
	reverse primer	CCAATGTCCAAGGGAGCCAC
Col 3α1	forward primer	TGGTCCTCAGGGTGTAAAGG
	reverse primer	GTCCAGCATCACCTTTTGGT
GAPDH	forward primer	ACCACAGTCCATGCCATCAC
	reverse primer	TCCACCACCCTGTTGCTGTA
IL-13	forward primer	GGAGCTGAGCAACATCACACA
	reverse primer	GGTCCTGTAGATGGCATTGCA
Smad7	forward primer	GTGTTGCTGTGAATCTTACG
	reverse primer	AGAAGAAGTTGGGAATCTGA